An Armadillo motif in Ufd3 interacts with Cdc48 and is involved in ubiquitin homeostasis and protein degradation

Gang Zhao[a,b], Guangtao Li[b], Hermann Schindelin[c], and William J. Lennarz[b,1]

[a]Center for Structural Biology and [b]Department of Biochemistry and Cell Biology, Stony Brook University, Stony Brook, NY 11794-5215; and [c]Rudolf Virchow Center for Experimental Biomedicine and Institute of Structural Biology, University of Würzburg, Versbacher Strasse 9, 97078 Würzburg, Germany

Contributed by William J. Lennarz, August 3, 2009 (sent for review May 14, 2009)

The yeast AAA-ATPase Cdc48 and the ubiquitin fusion degradation (UFD) proteins play important, evolutionarily conserved roles in ubiquitin dependent protein degradation. The N-terminal domain of Cdc48 interacts with substrate-recruiting cofactors, whereas the C terminus of Cdc48 binds to proteins such as Ufd3 that process substrates. Ufd3 is essential for efficient protein degradation and for maintaining cellular ubiquitin levels. This protein contains an N-terminal WD40 domain, a central ubiquitin-binding domain, and a C-terminal Cdc48-binding PUL domain. The crystal structure of the PUL domain reveals an Armadillo repeat with high structural similarity to importin-α, and the Cdc48-binding site could be mapped to the concave surface of the PUL domain by biochemical studies. Alterations of the Cdc48 binding site of Ufd3 by site-directed mutagenesis resulted in a depletion of cellular ubiquitin pools and reduced activity of the ubiquitin fusion degradation pathway. Therefore, our data provide direct evidence that the functions of Ufd3 in ubiquitin homeostasis and protein degradation depend on its interaction with the C terminus of Cdc48.

In eukaryotes, protein degradation is largely mediated by the ubiquitin-proteasome pathway. Intracellular proteins targeted for degradation are recognized by ubiquitin ligases and are tagged with chains of the small and highly conserved protein ubiquitin (1, 2). Coordinated by a series of ubiquitin-binding proteins, the multiubiquinated substrates are delivered to the proteasome for degradation (3). Ubiquitination usually involves the formation of an isopeptide bond between the C terminus of ubiquitin and the ε-amino group of an internal lysine residue of the substrate, or the preceding ubiquitin. Attachment of ubiquitin to the N-terminal residue of a protein also efficiently targets it for proteasomal degradation (4). Using the fusion protein Ub-Pro-β-galactosidase as substrate, the ubiquitin fusion degradation pathway (UFD) was identified in a yeast genetic screen (5). This screen revealed five UFD proteins (Ufd1–5) that were shown to participate in the ubiquitin-proteasome pathway. Ufd1 is involved in the dislocation and recruitment of ERAD (ER-associated protein degradation) substrates (6). Ufd2 has both ubiquitin protein ligase (E3) and ubiquitin chain elongation (E4) activities (7, 8). The detailed function of Ufd3 is still not clear, except deletion of this gene depletes the cellular pool of free ubiquitin (5). Ufd4 is a proteasome-associated ubiquitin E3 ligase (9), and Ufd5 (also known as Rpn4) controls the expression of genes encoding subunits of the proteasome (10).

Although not identified in the original UFD screen, the yeast AAA ATPase Cdc48 (known as p97 in mammals) has been shown to play an important role in the ubiquitin-proteasome system. Earlier it was proposed that Cdc48 organizes a cytosolic protein-degradation complex, which collects ubiquitinated substrates either from the endoplasmic reticulum or from the cytosol, and then delivers the substrates to the proteasome for degradation (3, 11). Interestingly, three Ufd proteins are involved in this pathway by directly interacting with Cdc48. Ufd1, together with Npl4, binds to the N-terminal domain of Cdc48 and is one of the best-studied substrate recruiting cofactors of Cdc48 (6, 12, 13). Ufd2 and Ufd3 are substrate-processing cofactors of Cdc48 that bind to a region other than its N-terminal domain (14, 15). In the case of Ufd3, it was demonstrated that it binds to the C terminus of Cdc48 (15). Ufd2 and Ufd3 compete for binding to Cdc48, suggesting a common binding site. Both of their interactions with Cdc48 depend on Ufd1 (14), thus suggesting a crosstalk between the substrate-recruiting and the substrate-processing cofactors of Cdc48.

In addition to protein degradation, Ufd3 has also been shown to function in the DNA damage response, the monoubiquitination of histone H2B, and the targeting of ubiquitinated membrane proteins to multivesicular bodies (16, 17). Most of Ufd3's function depends on its role in maintaining the cellular ubiquitin concentration (5, 16, 17). However, since no enzymatic activity has been found in Ufd3, the mechanism of ubiquitin depletion in the Ufd3 deletion mutants is not clear. Ufd3 could function by cooperating with a deubiquitinase, or by counteracting the function of Ufd2 (14). Ufd3 is a modular protein containing a WD40 domain at its N terminus, which is presumably involved in protein-protein interactions (18), a central ubiquitin-binding domain termed PFU (19), and a C-terminal PUL domain that interacts with Cdc48 (19) (Fig. 1*A*). Therefore, identifying which domain(s) of Ufd3 is involved in ubiquitin homeostasis is important in understanding its detailed functions.

In this study, we used structural and biochemical techniques to investigate the detailed interaction between Ufd3 and Cdc48. We demonstrate that the C-terminal domain of Ufd3 contains an Armadillo repeat fold, which interacts with the C terminus of Cdc48. Interestingly, an internal segment of Ufd3 binds to the Armadillo motif, and may regulate the interaction between Ufd3 and Cdc48. The finding that the C terminus of Cdc48 binds to the PUL domain of Ufd3 confirms the hypothesis that the C terminus of Cdc48 plays an important role in modulating the activity of Cdc48. In addition, we observed that blocking the interaction of Ufd3 with Cdc48 in vivo depletes cellular ubiquitin and interferes with the degradation of UFD substrate. Therefore, these studies show that Ufd3 must physically interact with Cdc48 to function in ubiquitin stabilization and protein degradation.

Results and Discussion

Overall Structure of the PUL Domain of Yeast Ufd3. The C-terminal PUL domain of yeast Ufd3 has been shown to interact with Cdc48 (19). To provide detailed information on this interaction,

Author contributions: G.Z., G.L., H.S., and W.J.L. designed research; G.Z. and G.L. performed research; G.Z. and G.L. analyzed data; and G.Z., G.L., H.S., and W.J.L. wrote the paper.

The authors declare no conflict of interest.

Data deposition: The atomic coordinates have been deposited in the Protein Data Bank, www.pdb.org [PDB ID code 3GAE (PUL domain)].

[1]To whom correspondence should be addressed. E-mail: wlennarz@notes.cc.sunysb.edu.

This article contains supporting information online at www.pnas.org/cgi/content/full/0908321106/DCSupplemental.

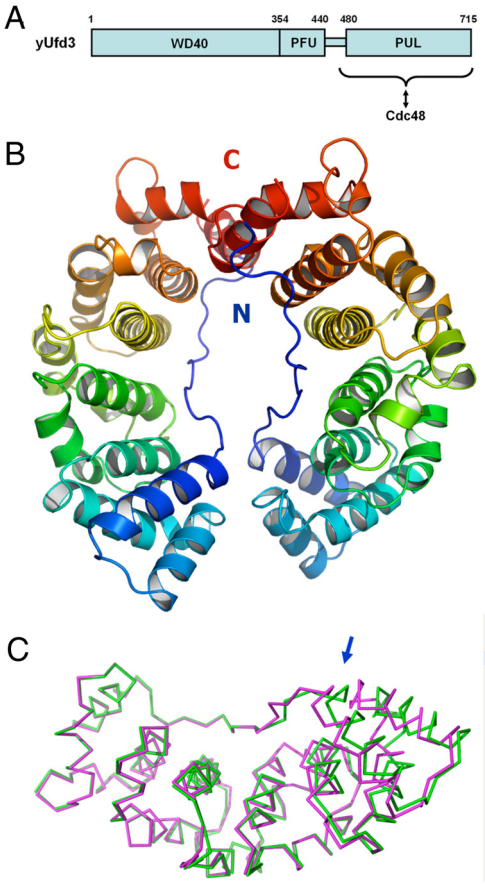

Fig. 1. Structure of the PUL domain. (*A*) Domain architecture of yeast Ufd3. The C-terminal domain used in the structural studies, which contains the PUL domain that binds directly to Cdc48, is indicated (*B*) Ribbon representation of the two PUL domains present in the asymmetric unit. Both chains are color coded form blue (N terminus) to red (C terminus). Figures describing the structure were prepared with PyMol (37). (*C*) Superposition of the two PUL domains which are shown as Cα-traces. The area with conformational differences between the PUL structures is indicated by the arrow.

the PUL domain of yeast Ufd3 (residues 464–715) was expressed, purified, and crystallized. The crystals were found to belong to space group $P3_1$ with two molecules in the asymmetric unit, even though the protein is monomeric in solution. The structure of the PUL domain (Fig. 1*B*) was solved by multiple isomorphous replacement and anomalous scattering. The structure was refined at 1.6-Å resolution, resulting in a final model with an R factor of 0.181 (R_{free} = 0.215). A representative simulated annealing F_o–F_c omit map contoured at 3σ is shown in Fig. S1, and the crystallographic data are summarized in Table 1 and Table S1. All of the residues are defined in the electron density maps and the model is of high quality according to the MolProbity program (20).

Even though the PUL domain of Ufd3 has no detectable sequence homology to any known structure, it folds into a structure containing Armadillo-repeats (21, 22) with six repeats, containing a total of 15 α-helices and no β-strands (Figs. 1*B* and 3*C*). Interestingly, the N-terminal 20 residues which are present mostly in extended conformation are oriented in an antiparallel fashion to the central axis of the Armadillo repeat and cover the concave surface of the PUL domain. The two molecules in the asymmetric unit have very similar structures, as they can be superimposed with a root mean square (rms) deviation in Cα atoms of 0.54 Å. Despite the overall similarity, significant differences are observed in the N-terminal four

Table 1. Refinement statistics

	PDB ID 3GAE
Resolution limits, Å	20.0–1.6
Number of reflections	67,543
Number of protein atoms	4,069
Number of solvent atoms	563
R (R_{free})	0.181 (0.215)
Deviations from ideal values in	
Bond distances, Å	0.020
Bond angles, °	1.756
Chiral volumes, Å^3	0.112
Planar groups, Å	0.009
Torsion angles	
Period 1, °	6.2
Period 2, °	37.9
Period 3, °	13.5
Ramachandran statistics (/)	
Favored	0.980
Allowed	0.998
Average B factors	
A, Å^2	12.7
B, Å^2	12.1
Solvent, Å^2	21.5

$R_{cryst}=\Sigma||F_o| - |F_c||/\Sigma|F_o|$ where F_o and F_c are the observed and calculated structure factor amplitudes. R_{free} is the same as R for 5% of the data randomly omitted from refinement. Ramachandran statistics indicate the fraction of residues in the most favored, additionally allowed, generously allowed and disallowed regions of the Ramachandran diagram as defined by MolProbity (20).

helices (α1–α4), where main chain atoms move up to 5 Å relative to each other, thus indicating structural flexibility in this region (Fig. 1*C*). This structural flexibility could be of functional significance if the N-terminal loop binds reversibly to the PUL domain (see below). If not mentioned otherwise, molecule A (depicted on the left side in Fig. 1*B*) was used in the structural analysis.

Comparison of the PUL Domain of Ufd3 with Other Proteins Containing Armadillo Repeats. The structure of the PUL domain was submitted to the DaliLite server to identify structural homologs (23). PUL was shown to most closely resemble the Armadillo repeat of importin-α with an rms deviation of 4.0 Å (Z score = 11.0) for 201 Cα-atoms (Fig. 2*A*). In contrast to the PUL domain, importin-α features 10 Armadillo repeats, of which repeats 1–6 correspond to the entire PUL domain. The Armadillo motif of importin-α binds to the nuclear localization signal (NLS) of proteins and results in their nuclear targeting (24).

Interestingly, a portion of yeast Ufd2, another cofactor in the ubiquitin fusion degradation pathway (5), was found to align with the PUL domain of Ufd3 with a Z score of 8.0 (Fig. 2*B*) using Dali (23). Although, the Cdc48 binding site on Ufd2 has not been determined unambiguously, yeast two hybrid data suggested that it is formed by residues 808–856 (3), which constitute the C-terminal end of the C-terminal region of the Armadillo repeats (8) (Fig. 2*B*). This assignment is only tentative since the possibility has to be considered that deleting residues 809–916 of Ufd2 (3) destroys the overall structure of the Armadillo-repeat domain, which then results in the observed Cdc48-binding defect. Ufd3 competes with Ufd2 for binding to Cdc48 (14), possibly indicating that the mode of their interactions with Cdc48 is similar. On the other hand, detailed structural alignment between the Armadillo domains of Ufd2 and Ufd3 showed that the proposed binding residues of Ufd3 (see below) do not present on the corresponding surface of Ufd2. Therefore, how Ufd2 binds to Cdc48 remains to be investigated. Besides Ufd2

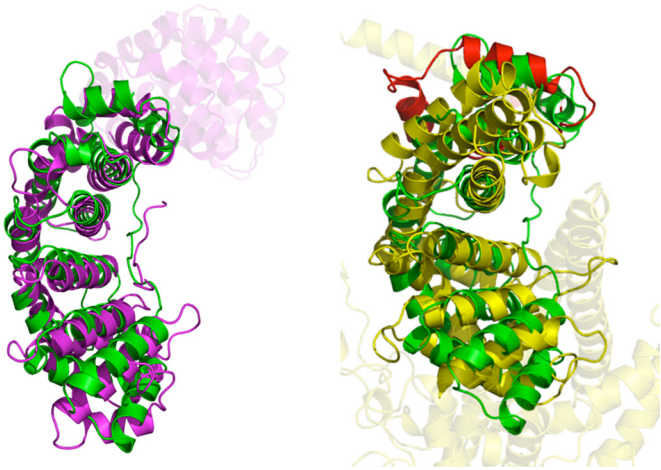

Fig. 2. Structural alignments of the Armadillo repeats of Ufd3 with importin-α (*A*) and Ufd2 (*B*). The superposition matrix of PUL with mouse importin-α (PDB ID: 1IAL) and yeast Ufd2 (PDB ID: 2QIZ) were calculated by DALI (23). The PUL domain structure is shown in the same orientation as in Fig. 1*B* and is colored green. The superposed regions of importin-α and Ufd2 are colored in solid magenta and yellow, respectively. The proposed Cdc48 binding site of Ufd2 (residues 808–856) (3) is highlighted in red.

and Ufd3, Armadillo repeats have been found in several other U-box containing proteins involved in protein ubiquitination and degradation, such as PUB14 in *Arabidopsis* (25). It is interesting to note that, in addition to the Armadillo motif, these proteins either have ubiquitin ligase activity, such as Ufd2 and PUB14, or have additional ubiquitin-binding domains, such as the PFU domain in Ufd3.

With the identification of an Armadillo repeat as the Cdc48-binding site in Ufd3, there are now two known distinct domain architectures that interact with the C terminus of Cdc48, namely, the Armadillo motif as demonstrated here and the PUB domain present in mammalian PNGase and other proteins (15, 26). Therefore, the ubiquitin mediated protein degradation pathway could be regulated by a complex protein interaction network, involving cooperative and/or competitive binding of various substrate processing cofactors, including Ufd2, Ufd3, and the PUB domain-containing proteins.

^{Ufd3}PUL Interacts with the C Terminus of Cdc48. The PUL domain is necessary and sufficient for the interaction of Ufd3 with Cdc48 and p97 (14, 15, 19). Unlike most other Cdc48/p97 cofactors, mouse Ufd3 binds to the C terminus of Cdc48/p97 (15). An isothermal titration calorimetry (ITC) experiment was carried out using the PUL domain of yeast Ufd3 and a chemically synthesized peptide consisting of the C-terminal 14 residues of yeast Cdc48. As shown in Table 2, yeast ^{Ufd3}PUL binds to the C terminus of Cdc48 with a molar ratio of 1:1 and a dissociation constant of 3.5 μM, which corresponds to the affinity determined earlier for the mouse protein (K_D = 4.1 μM) (15). It should be noted that PUL binds to the C terminus of Cdc48/p97 and to the hexameric full length protein with similar affinities (Fig. S2), suggesting that oligomerization of Cdc48/p97 does not affect its binding to Ufd3.

By comparing the sequences of the PUL domains from different species (Fig. S3), we observed that most of the conserved surface exposed residues are located near the concave side of the Armadillo repeat (Fig. 3*A*). If the N-terminal loop is ignored, two conserved patches are obvious on the surface of the PUL domain. As shown in Fig. 3*A*, the patch on the left side consists of residues Ile-620, Ala-621, Thr-624, Asn-628, Glu-665, Arg-669, and Val-672, whereas that on the

Table 2. Interaction between the wild type and mutant PUL proteins and the Cdc48 C-terminal peptide. (The T_m shift values are the average of two independent measurements and differ by less than 0.5°C)

PUL Proteins	N	K_D, μM	ΔT_m, °C
W.T.	0.95	3.5 ± 0.7	3.5
N491A	0.88	3.5 ± 0.2	4.0
D538A	0.88	13.9 ± 2.7	3.0
R541A	n.d.*	n.d.*	0
K545A	0.85	3.3 ± 0.5	3.5
N578A	0.92	35.7 ± 3.2	1.0
I620A	0.91	4.4 ± 0.6	4.0
T624A	1.05	9.6 ± 3.0	2.0
E665A	1.04	4.6 ± 0.7	3.0
R669A	1.0**	83.3**	1.0
V672A	0.93	12.8 ± 2.3	1.5

*n.d.: not detected
**: The ITC binding curve was fitted by restraining the N value to 1.0.

right side is formed by Asp-538, Arg-541, Leu-542, Lys-545, and Asn-578. We hypothesize that these regions of the PUL domain contain the Cdc48-binding site based on sequence conservation and the following observations. First, the concave surface represents the primary protein binding site of the Armadillo domain (27). Second, this area of PUL forms a continuous positively charged electrostatic surface (Fig. 3*B*), which would be expected to complement the highly negatively charged C terminus of Cdc48.

To test this hypothesis, a site-directed mutagenesis approach

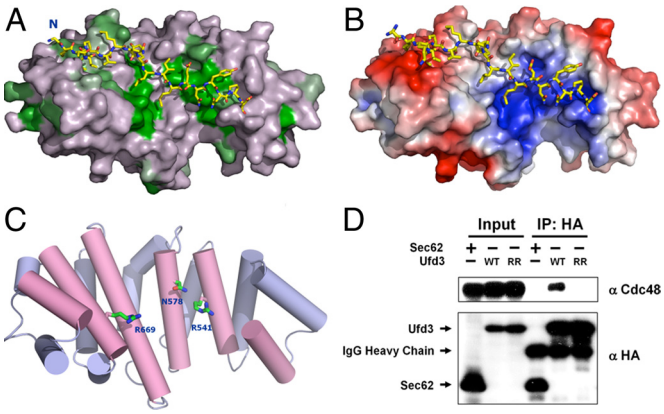

Fig. 3. PUL domain sequence conservation. (*A*) Surface representation of the PUL domain with conserved residues highlighted in green and the N-terminal peptide in stick representation. The N terminus of the protein is indicated and the same orientation of the structure is used in panels *C* and *D*. (*B*) PUL domain electrostatic surface potential (blue, electropositive, and red, electronegative). The electrostatic surface potential of PUL excluding the N-terminal peptide (shown in all bonds representation) was calculated using APBS (38) assuming an ionic strength of 0.1 M. Surface representation of the PUL domain is color coded according to its electrostatic surface potential (blue, electropositive and red, electronegative). (*C*) The proposed Cdc48 binding region is on the concave face of the PUL Armadillo repeats. Residues Arg-541, Asn-578, and Arg-669 are involved in binding to Cdc48 and are shown in sticks representation. The six α-helices (each representing one Armadillo repeat), that comprise the concave side of the PUL domain are shown in pink. The helices on the convex side are colored in light blue. (*D*) Co-immunoprecipitation experiments showed that the R541A/R669A mutant of Ufd3 (RR) does not bind to Cdc48 in vivo. Equal amount of YH-2, ufd3 deletion strain carrying WT ufd3 and RR mutant were used for IP experiment with EZview Red Anti-HA Affinity Gel. The whole cell lysate (Input) and the proteins bound on the affinity Gel were subjected to electrophoresis, transfer and immunoblot with either Cdc48 or HA antibody.

was used to analyze the importance of these conserved residues in Ufd3 for Cdc48 binding. The above mentioned conserved residues of Ufd3 were singly mutated to Ala. Except for the N628A mutant, which when overexpressed was localized to inclusion bodies, all other proteins were overexpressed in soluble form and could be purified as monomers based on size exclusion chromatography. Circular dichroism experiments with the mutant proteins showed typical spectra characteristic of α-helical proteins that were nearly identical to the wild type. The thermostability of the mutants was analyzed by using differential scanning fluorimetry (DSF) (28), and the proteins were found to exhibit distinct melting curves with a melting temperature (T_m) above 46 °C, thus suggesting that the mutations do not perturb the overall protein conformation.

We assessed the interaction between ^{Ufd3}PUL and Cdc48 by ITC and DSF (Fig. S4 and Table 2). Upon binding of the peptide, the T_m of the wild-type PUL protein was increased by approximately 3.5 °C (Table 2). The PUL mutants were analyzed under the same conditions and a smaller T_m shift would indicate weaker peptide binding. The R541A mutant did not have any detectable binding with Cdc48 in both the ITC and the DSF experiments (Table 2). Other defective mutants include R669A and N578A, which showed much reduced binding affinity with Cdc48 and also smaller T_m shift. We propose that these residues constitute the Cdc48 binding site on the PUL domain (Fig. 3*C*). The positively charged residues R541 and R669 of Ufd3 could interact with the highly negatively charged C terminus of Cdc48, whereas residue N578 could be involved in hydrogen bonding. To confirm that residues R541 and R669 are important for the binding of Ufd3 to Cdc48 in vivo, co-immunoprecipitation experiments were carried out in wild type and the Ufd3-R541A/R669A mutant yeast strains. Western blot analysis showed that the double mutation does not affect the amount of the Ufd3 protein in the cells. Consistent with our biochemical data, the R541A/R669A mutant failed to interact with Cdc48 in vivo (Fig. 3*D*).

Similarities in the binding affinity and the fact that both the C terminus of Cdc48/p97 and the Cdc48-binding residues of Ufd3 are highly conserved suggest that binding of Ufd3 to Cdc48 is conserved from yeast to mammals. The C terminus of mouse Cdc48 homolog p97 (with the sequence TEDNDDDLYG-COOH) also interacts with the PUB domain (15, 26). Even though the mouse PUB and PUL domains interact with Cdc48/p97 with similar affinities, it seems that the mode of interaction is different. First, the PUB domain is structurally different from the PUL domain. Second, the PUB domain most extensively interacts with the last three residues of p97, namely, Leu-804, Tyr-805, and Gly-806, through hydrophobic interaction and hydrogen bonds (15). In contrast, the interaction of the PUL domain with Cdc48 appears to be largely through salt bridges with the upstream negatively charged residues of the protein. In addition, the C-terminal 10 residues of Cdc48/p97 are sufficient for interacting with the PUB domain. On the other hand, even though Ufd3 binds to the last 10 residues of Cdc48, it interacts with the last 13 residues of Cdc48/p97 with a much higher affinity (K_d = 2 μM) (Fig. S2).

The Ufd3-Cdc48 Interaction Is Required for Efficient Protein Degradation. To assess the role of the PUL domain in the protein degradation pathway in vivo, degradation of the model UFD substrate Ub-proline-β-galactosidase (Ub-Pro-βGal) was measured in the wild-type and the Ufd3 mutant yeast strains (5). In agreement with previous studies (5), we found that compared to the wild type, deletion of Ufd3 significantly slowed down the degradation of Ub-Pro-βGal, resulting in an increased β-galactosidase activity in the cells (Fig. 4). Both the R541A and R669A single mutants and especially the R541A/R669A double mutant inhibit the degradation of Ub-Pro-βGal

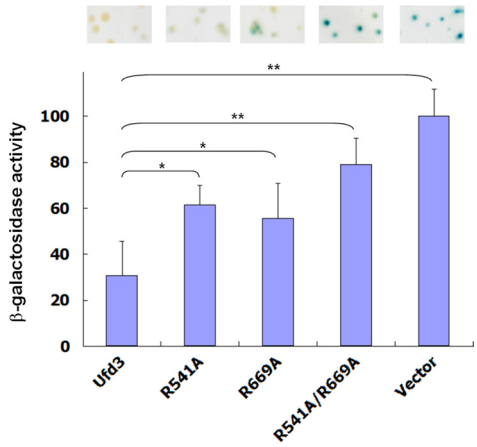

Fig. 4. Degradation of Ub-Pro-βGal. Equal amount of yeast cells co-expressing Ub-Pro-βGal and wild-type Ufd3 or the indicated Udf3 mutants were lysed and the β-galactosidase activity was measured using a kit from Pierce. (*) and (**) represent *P* values <0.05 and <0.005, respectively, between the yeast Ufd3 mutants and the wild type cells. Images from the β-galactosidase filter assay are shown on the top in the same order as the corresponding columns.

as reflected in a significantly higher activity of β-galactosidase than that in the wild type. These results suggest that the interaction between Ufd3 and Cdc48 plays an important role in the protein degradation pathway.

The Ufd3-Cdc48 Interaction Is Required for Maintaining Cellular Ubiquitin Levels. Even though no enzymatic activity has been detected for Ufd3, deletion of Ufd3 results in depletion of the cellular ubiquitin pool (5). We wondered whether the interaction between Ufd3 and Cdc48 is important for ubiquitin homeostasis. The turn-over rates of ubiquitin in the Ufd3 mutants defective in Cdc48 binding were compared to those in the wild-type (Fig. 5). Ubiquitin in the wild type is stable for up to 1 h, whereas it rapidly decayed in the Ufd3 deletion mutant, in agreement with previous studies (5). The R669A mutant did not affect the degradation of ubiquitin very much, probably due to residual

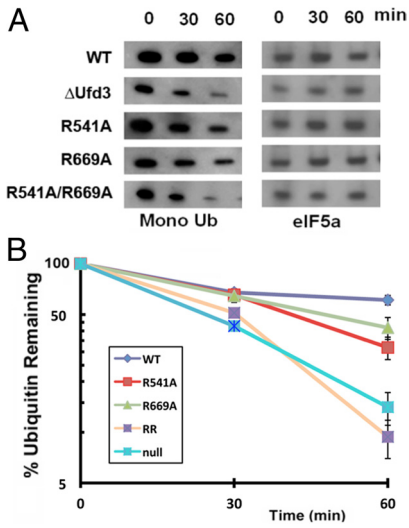

Fig. 5. Free ubiquitin is depleted more rapidly in the Ufd3 mutants. Equal amount of the indicated yeast mutant strains were collected at the indicated time points and subjected to immunoblot with either ubiquitin or eIF5a antibody as a loading control. Quantification of the blot is shown in the lower panel. RR represents the R541A/R669A double mutant.

binding of this mutant to Cdc48 (Fig. S4*A* and Table 2). In contrast, the R541A mutation somewhat increased the ubiquitin degradation and, even more strikingly, ubiquitin in the R541A/R669A double mutant was turned over as rapidly as in the deletion mutant. This finding suggests that the direct interaction between Ufd3 and Cdc48 is important for ubiquitin homeostasis in the cells. Cdc48 and Ufd3 are highly conserved from yeast to mammals, and we consequently hypothesize that in mammals the interaction between p97 and the Ufd3 homolog PLAP (phospholipase A2-activating protein) has a similar function. It has been shown that deletion of deubiquitinases results in ubiquitin depletion, probably due to the degradation of polyubiquitin chains by the proteasome (29). Even though Ufd3 has not been described to have deubiquitinase activity, it has been shown to cooperate with the deubiquitinating enzyme OTU1 (14). Furthermore, it could recruit other deubiquitinases through its N-terminal WD40 domain, or prevent multiubiquitination by counteracting the ubiquitin ligase activity of Ufd2. Ufd3 has been shown to be involved in ubiquitin dependent protein degradation, the DNA damage response, phospholipase activation and the targeting of ubiquitinated membrane proteins to multivesicular bodies (5, 16, 17, 30). Whether these functions depend on the interaction between Ufd3 and Cdc48 will be the subject of future studies.

The Interaction Between Cdc48 and Ufd3 May Be Autoinhibitated by the Internal Loop. In mammals, the binding of importin-α to the NLS of nuclear proteins is autoinhibited by an internal NLS sequence of importin-α which binds to the NLS binding site located in the Armadillo repeats (31) (Fig. 2*A*). In the cytosol, importin-α binds to importin-β and this interaction prevents the binding of the internal NLS of importin-α to its Armadillo repeats and converts it to the high-affinity form (31). Once transported into the nucleus, importin-α dissociates from importin-β and is autoinhibited again (24). Similar to the structure of mouse importin-α (PDB ID: 1IAL), we found that an internal loop of Ufd3 binds extensively to the concave surface of the Armadillo core of the protein and covers its Cdc48-binding site (Fig. 2*A*). Based on these observations, we propose a similar autoregulatory role of the loop region of Ufd3 in its interaction with Cdc48. We envisage that recognition of the polyubiquitinated substrates by the upstream PFU domain of Ufd3 may alter the conformation of the loop region, which will expose the Cdc48-binding site for more efficient binding. In an alternative mechanism the C terminus of Cdc48/p97 could bind adjacent to the N-terminal loop region of the PUL domain, possibly inducing a conformational change in the loop, as seen in the Armadillo-repeat containing and pheromone-binding PrgX transcriptional repressor protein (32). Either mechanism could result in conformational changes in Ufd3 that modulate its capacity as a substrate-processing cofactor. Further studies on these mechanisms may shed light on the function of Ufd3 and will provide valuable information on how the ubiquitin degradation pathway is regulated.

Materials and Methods

Protein Purification and Crystallization. The yeast PUL domain proteins (residues 464–715 of Ufd3) were overexpressed and purified from BL21(DE3) Codon Plus RIL cells (Stratagene) (see *SI Text*).

Crystals of the yeast PUL protein were grown by using the hanging drop diffusion method against a reservoir solution containing 0.1 M sodium acetate (pH 5.6), 0.1 M $MgCl_2$ and 26–28% PEG 3350 at 18 °C. The heavy atom derivatives were prepared by soaking the crystals in either 10 mM sodium ethylmercurithiosalicylate for 30 min or 0.5 M sodium iodide for 1 min. Crystals were transferred into mother liquor supplemented with 10% glycerol and cryocooled by rapid immersion in liquid nitrogen to allow data collection at 100 K. Diffraction data of the heavy atom derivatives were collected using a Rigaku RU-H3RHB rotating anode generator equipped with an R-AXIS IV^{++} imaging plated detector and confocal optics in the Center for Structural Biology at Stony Brook University. Native datasets were collected on beam line X26C of the National Synchrotron Light Source (NSLS) at Brookhaven National Laboratory (BNL) on an ADSC Quantum-4 detector. Diffraction data were indexed, integrated and scaled with HKL2000 (33). The structure analysis was complicated by the fact that the crystals had a high tendency to be merohedrally twinned. Both of the derivative data sets displayed a twinning level of around 25%. Initial phases were determined by multiple isomorphous replacement and anomalous scattering (MIRAS) with Sharp/AutoSharp (34) from which an electron density map showing clear helical features could be obtained. The structure model was build in Coot (35) and refined by using Refmac (36) against a non-twinned native dataset at 1.6-Å resolution, thus ultimately overcoming all complications due to twinning.

ITC Experiments. Isothermal titrations were carried out on a VP-ITC microcalorimeter (MicroCal). A peptide corresponding to the C-terminal 14 residues of yeast Cdc48 was chemically synthesized by Anaspec. Before each experiment, the proteins and peptide were dialyzed overnight at 4 °C against TBS buffer containing 20 mM Tris·HCl (pH 8.5) and 150 mM NaCl. Proteins at concentrations of approximately 15 μM were titrated with 0.2 mM of peptide at 25 °C. The binding parameters were calculated by fitting the data to a single site binding model using the MicroCal Origin software.

Differential Scanning Fluorimetry. The thermostability of the mutant proteins was assayed on a Bio-Rad DNA Engine Opticon 2 real-time PCR cycler (28). Samples of 50 μL containing 0.2 mg/mL protein and 5$\times$ Sypro Orange dye (Invitrogen) in TBS buffer were prepared in thin-walled PCR plates (MJ Research). For the melting temperature (T_m) shift assays, 0.75 mM of the yeast Cdc48 peptide (corresponding to a 100-fold molar concentration of the protein) was included in the reaction mixtures. The fluorescence intensities were determined at 0.5-°C intervals over the temperature range from 20 to 95 °C. The T_m values were calculated using the Opticon Monitor software from Bio-Rad.

Coimmunoprecipitation Experiments. Ufd3 yeast knock out strain (Open Biosystems), was transformed with pRS315 plasmids harboring either wild-type or mutant Ufd3 genes, which were tagged with 3$\times$HA at the C terminus. A YH-2 strain (kindly provided by Dr. Y. Harada, Stony Brook University) in which Sec62 is tagged with triple HA was used as a negative control. The cells were lysed by using a bead beater in the lysis buffer (100 mM NaCl, 50 mM Tris-HCl, pH 7.5, 5 mM $MgAc_2$, 1 mM EDTA, 5% glycerol, protease inhibitors, and 0.3% Triton X-100). The total cell lysate was precleared for 2 h at 4 °C by adding 20 μL Protein G agarose beads (Invitrogen). After preclearing, 20 μL EZview Red Anti-HA Affinity Gel (Sigma) were added to the cell lysate. The binding experiments were performed at 4 °C for 2 h, after which the beads were washed three times with lysis buffer with 1% Triton X-100. Bound proteins were eluted with SDS sample buffer and analyzed by SDS/PAGE followed by western blot analysis with monoclonal antibody against HA or polycolonal antibody against Cdc48 (generously provided by T. Sommer at Max-Delbrück Center for Molecular Medicine, Berlin-Buch, Germany).

Ub-Proline-β-Galactosidase Activity Assay. The yeast Ufd3-null strain was co-transformed with Ub-Pro-βGal [a generous gift from D. Finley (Harvard Medical School)] and either the pRS315 vector or the Ufd3 expression vectors. Cells were grown overnight at 30 °C in -His/-Ura/Raffinose SD media, and the expression of Ub-Pro-βGal was induced by adding 2% galactose for 6 h. The β-galactosidase activity of the cells was measured using the yeast β-galactosidase assay kit (Pierce) according to the manufacturer's protocol. Standard deviations were determined from four independent measurements. The degradation of Ub-Pro-βGal was also measured using the β-galactosidase filter assay. Briefly, yeast colonies on the -His/-Ura/Raffinose plates were transferred onto a nitrocellulose filter and lysed in liquid nitrogen. The activity of the β-galactosidase was measured by incubating the filter in X-gal reaction buffer overnight at 30 °C.

Ubiquitin Turnover Assay. The analysis was carried out as described earlier (14). The yeast Ufd3 mutant strains were grown to an A_{600} of 1. After cycleohexamide was added at a final concentration of 200 μg/mL, equal amounts of cells were collected at the indicated time points and boiled in SDS loading buffer. The samples were immunoblotted with either anti-ubiquitin or anti-eIF5a antibody. The blot was scanned and the amounts of remaining free ubiquitin were quantified and normalized to eIF5a.

ACKNOWLEDGMENTS. We thank the beamline scientists at the National Synchrotron Light Source at Brookhaven National Laboratory for diffrac-

tion data collection; Mrs. L. Li and Mrs. A. Havado (Stony Brook University) for technical assistance; Dr. Y. Harada (Stony Brook University) for materials and discussions on the manuscript; Dr. T. Sommer for the Cdc48 antibody; and Dr. D. Finley for reagents. This work was supported by National Institutes of Health Grants GM33814 (to W.J.L.) and DK54835 (to H.S.) and Deutsche Forschungsgemeinschaft FZ 82 (to H.S.).

1. Hershko A, Ciechanover A (1998) The ubiquitin system. *Annu Rev Biochem* 67:425–479.
2. Pickart CM (2001) Mechanisms underlying ubiquitination. *Annu Rev Biochem* 70:503–533.
3. Richly H, et al. (2005) A series of ubiquitin binding factors connects CDC48/p97 to substrate multiubiquitylation and proteasomal targeting. *Cell* 120:73–84.
4. Bachmair A, Finley D, Varshavsky A (1986) In vivo half-life of a protein is a function of its amino-terminal residue. *Science* 234:179–186.
5. Johnson ES, Ma PC, Ota IM, Varshavsky A (1995) A proteolytic pathway that recognizes ubiquitin as a degradation signal. *J Biol Chem* 270:17442–17456.
6. Ye Y, Meyer HH, Rapoport TA (2003) Function of the p97-Ufd1-Npl4 complex in retrotranslocation from the ER to the cytosol: Dual recognition of nonubiquitinated polypeptide segments and polyubiquitin chains. *J Cell Biol* 162:71–84.
7. Koegl M, et al. (1999) A novel ubiquitination factor, E4, is involved in multiubiquitin chain assembly. *Cell* 96:635–644.
8. Tu D, Li W, Ye Y, Brunger AT (2007) Inaugural article: Structure and function of the yeast U-box-containing ubiquitin ligase Ufd2p. *Proc Natl Acad Sci USA* 104:15599–15606.
9. Xie Y, Varshavsky A (2000) Physical association of ubiquitin ligases and the 26S proteasome. *Proc Natl Acad Sci USA* 97:2497–2502.
10. Xie Y, Varshavsky A (2001) RPN4 is a ligand, substrate, and transcriptional regulator of the 26S proteasome: A negative feedback circuit. *Proc Natl Acad Sci USA* 98:3056–3061.
11. Li G, Zhao G, Zhou X, Schindelin H, Lennarz WJ (2006) The AAA ATPase p97 links peptide N-glycanase to the endoplasmic reticulum-associated E3 ligase autocrine motility factor receptor. *Proc Natl Acad Sci USA* 103:8348–8353.
12. Jentsch S, Rumpf S (2007) Cdc48 (p97): A ''molecular gearbox'' in the ubiquitin pathway? *Trends Biochem Sci* 32:6–11.
13. Isaacson RL, et al. (2007) Detailed structural insights into the p97-Npl4-Ufd1 interface. *J Biol Chem* 282:21361–21369.
14. Rumpf S, Jentsch S (2006) Functional division of substrate processing cofactors of the ubiquitin-selective Cdc48 chaperone. *Mol Cell* 21:261–269.
15. Zhao G, et al. (2007) Studies on peptide:N-glycanase-p97 interaction suggest that p97 phosphorylation modulates endoplasmic reticulum-associated degradation. *Proc Natl Acad Sci USA* 104:8785–8790.
16. Lis ET, Romesberg FE (2006) Role of Doa1 in the *Saccharomyces cerevisiae* DNA damage response. *Mol Cell Biol* 26:4122–4133.
17. Ren J, Pashkova N, Winistorfer S, Piper RC (2008) DOA1/UFD3 plays a role in sorting ubiquitinated membrane proteins into multivesicular bodies. *J Biol Chem* 283:21599–21611.
18. Neer EJ, Schmidt CJ, Nambudripad R, Smith TF (1994) The ancient regulatory-protein family of WD-repeat proteins. *Nature* 371:297–300.
19. Mullally JE, Chernova T, Wilkinson KD (2006) Doa1 is a Cdc48 adapter that possesses a novel ubiquitin binding domain. *Mol Cell Biol* 26:822–830.
20. Davis IW, et al. (2007) MolProbity: all-atom contacts and structure validation for proteins and nucleic acids. *Nucleic Acids Res* 35:W375–383.
21. Hatzfeld M (1999) The armadillo family of structural proteins. *Int Rev Cytol* 186:179–224.
22. Peifer M, Berg S, Reynolds AB (1994) A repeating amino acid motif shared by proteins with diverse cellular roles. *Cell* 76:789–791.
23. Holm L, Kaariainen S, Rosenstrom P, Schenkel A (2008) Searching protein structure databases with DaliLite v. 3. *Bioinformatics* 24:2780–2781.
24. Weis K (1998) Importins and exportins: How to get in and out of the nucleus. *Trends Biochem Sci* 23:185–189.
25. Andersen P, et al. (2004) Structure and biochemical function of a prototypical *Arabidopsis* U-box domain. *J Biol Chem* 279:40053–40061.
26. Madsen L, et al. (2008) Ubxd1 is a novel co-factor of the human p97 ATPase. *Int J Biochem Cell Biol* 40:2927–2942.
27. Conti E, Uy M, Leighton L, Blobel G, Kuriyan J (1998) Crystallographic analysis of the recognition of a nuclear localization signal by the nuclear import factor karyopherin alpha. *Cell* 94:193–204.
28. Niesen FH, Berglund H, Vedadi M (2007) The use of differential scanning fluorimetry to detect ligand interactions that promote protein stability. *Nat Protoc* 2:2212–2221.
29. Leggett DS, et al. (2002) Multiple associated proteins regulate proteasome structure and function. *Mol Cell* 10:495–507.
30. Clark MA, et al. (1991) Cloning of a phospholipase A2-activating protein. *Proc Natl Acad Sci USA* 88:5418–5422.
31. Kobe B (1999) Autoinhibition by an internal nuclear localization signal revealed by the crystal structure of mammalian importin alpha. *Nat Struct Biol* 6:388–397.
32. Kozlowicz BK, et al. (2006) Molecular basis for control of conjugation by bacterial pheromone and inhibitor peptides. *Mol Microbiol* 62:958–969.
33. Otwinowski Z, Minor W (1997) in *Processing of X-ray Diffraction Data Collected in Oscillation Mode* (Academic press, New York), pp 307–326.
34. Vonrhein C, Blanc E, Roversi P, Bricogne G (2007) Automated structure solution with autoSHARP. *Methods Mol Biol* 364:215–230.
35. Emsley P, Cowtan K (2004) Coot: Model-building tools for molecular graphics. *Acta Crystallogr D Biol Crystallogr* 60:2126–2132.
36. Murshudov GN, Vagin AA, Dodson EJ (1997) Refinement of macromolecular structures by the maximum-likelihood method. *Acta Crystallogr D Biol Crystallogr* 53:240–255.
37. DeLano WL (2002) in *The PyMOL User's Manual* (DeLano Scientific, Palo Alto, CA).
38. Baker NA, Sept D, Joseph S, Holst MJ, McCammon JA (2001) Electrostatics of nanosystems: Application to microtubules and the ribosome. *Proc Natl Acad Sci USA* 98:10037–10041.